The Method of Regularization and its Application to Some EM Problems

Ayhan Altintaş[1] and Alexander I. Nosich[2]

[1] Department of Electrical and Electronics Engineering, Bilkent University, 06533 Bilkent, Ankara, Turkey
[2] Institute of Radiophysics and Electronics Ukrainian Academy of Sciences, 310085, Kharkov, Ukraine

Abstract. The regularization of the integral equations for the solution of electromagnetic problems is discussed. The technique includes a semi-analytic inversion of the integral operator resulting in equation of the Fredholm second kind, which can be solved using numerical inversion. The procedure is employed through Riemann-Hilbert Problem technique for the electromagnetic problems that can be put into a dual-series equation form. An example of the method is described for the E-wave scattering from a cavity-backed aperture.

Keywords. Regularization, electromagnetic scattering, Riemann-Hilbert problem, cavity-backed apertures

1 Introduction

Scattering, diffraction and radiation of electromagnetic waves can be reduced to integral equations using generalized potential theory approach. Analytical solution of these integral equations is possible only for some classes of problems. The Wiener-Hopf approach is one of the powerful analytical techniques for the 2-D problems [1]. On the other hand, purely numerical methods have been developed and widely used in all kinds of problems. In between these approaches are the numerical-analytical techniques that are based on the partially analytical development of the solution and calculation of the final result through numerical methods. Here, partial inversion of the singular kernel of the integral equation plays an important role to convert the problem into a form that can be solved numerically in an efficient and accurate way.

For an operator L, the approach inverts the singular part of the operator equation

$$L\rho = f \tag{1}$$

so that one gets

$$(I + L_1^{-1}L_2)\rho = L_1^{-1}f \tag{2}$$

where I is the identity operator, L_1 is the singular part of the operator L, and L_1^{-1} is its inverse. It is obvious to note that $L = L_1 + L_2$. The above equation can also be written in compact form as

$$(I - K)\rho = S \qquad (3)$$

where $K = -L_1^{-1}L_2$ and $S = L_1^{-1}f$.

The advantage gained in converting (1) into a form given in (3) is the compact nature of the operator K which then implies that the operator equation (1) is of Fredholm second kind. The existence of the solution is guaranteed and numerical approximation is mathematically rigorous. For this reason, this process is called the regularization of the operator equation. The subtlety lies in identification of the singular part of the operator and its analytical inversion.

For problems involving circular strips or periodic grating of strips, the regularization can be done through Riemann-Hilbert Problem (RHP) approach which utilizes the theory of analytic functions of complex variable ([2-4]). This approach has been widely exploited especially in the former Soviet Union for the scattering from a wide class of periodic, zero-thickness, 2-D scatterers with perfect conductivity. Initially, the focus was on the analysis of strip gratings, later circular open screens or a collection of such screens in various environments have been analyzed. An extensive list of such works is given in [3].

The common nature of all these problems is that the boundary conditions allow the solution to be formulated in the form of dual series equations. The RHP solution of dual series equations was introduced into the Western literature by Ziolkowsky ([5-7]). Later, E - and H - wave scattering from coated cavities have been explored ([8, 9]). Recently, a complex source point-dual series combination has lead to the RHP formulation of the radiation from reflector antennas [10, 11]. For cavity structures, a comparative study of the method of regularization and the Wiener-Hopf is given in [12]. In the following sections, the dual series equations and their regularization through RHP will be described for scattering from cavity-backed apertures (CBA). For a complete discussion of the subject, the reader is referred to [3].

2   The RHP Technique

Consider a simple, smooth, non-intersecting closed curve C in the complex plane of variable $z = x + iy$ and define the open domains exterior and interior to C as Q^+, and Q^-, respectively. Let the closed curve C be composed of two curves M and N such that

$$C = M \cup N. \qquad (4)$$

Consider a boundary value problem concerning the reconstruction of a complex function $X(z)$ satisfying

$$X^+(z_o) + X^-(z_o) = B(z_o); \quad z_o \in M \tag{5}$$

$$X^+(z_o) - X^-(z_o) = 0; \qquad z_o \in N \tag{6}$$

where $X^+(z_o)$ and $X^-(z_o)$ are the limiting values of $X(z)$ from outside and from inside of C, respectively. $B(z_o)$ is a given function which is Hölder continuous. The Riemann-Hilbert Problem is the determination of $X(z)$ satisfying the above equations and the condition that $X(z)$ is vanishing as $|z| \to \infty$. Guided by the assumption that $X(z)$ has singularities of order 1/2 at each of two endpoints of M (this is a necessity for the electromagnetic problems due to edge condition), one can introduce a characteristic function $R(z)$ of the problem under consideration, such that $R(z)X(z)$ is regular in the whole plane. The procedure is described in [3] and introduces

$$R(z) = (z - a_1)^{1/2}(z - a_2)^{1/2} \tag{7}$$

with $z = a_{1,2}$ at the endpoints and the branch is chosen so that the limits differ by sign: if $z \in Q^{\pm}$ and $z_o \in C$, then for $z \to z_o$, $R(z) \to R^{\pm}(z_o) = \pm R(z_o)$. Now, by introducing a new function

$$Y(z) = X(z)R(z) \tag{8}$$

one obtains

$$Y^+(z_o) - Y^-(z_o) = D(z_o); \quad z_o \in C \tag{9}$$

where

$$D(z_o) = \begin{cases} B(z_o)R^+(z_o), & z_o \in M \\ 0, & z_o \in N. \end{cases} \tag{10}$$

The solution of the above RHP is given in the form of Cauchy integral

$$Y(z) = \frac{1}{2\pi i} \int_C \frac{D(z_o)dz_o}{z_o - z} + G \tag{11}$$

where G is a constant which has to be determined from physical conditions of the problem. Rewriting (11) for the function $X(z)$, one gets

$$X(z) = \frac{1}{2\pi i} \frac{1}{R(z)} \int_C \frac{B(z_o)R^+(z_o)dz_o}{z_o - z} + \frac{G}{R(z)}. \tag{12}$$

In the dual series solution applications, the value of the function $X(z)$ exactly on the curve is requested. For such cases, one uses the Plemelj-Sokhotskii formulas for the limiting values of $X(z)$ on M to obtain

$$X^+(z_o) - X^-(z_o) = \frac{1}{\pi i} \frac{1}{R^+z_o} \int_M \frac{B(z_o)R^+(z_o)dz_o}{z_o - z} + \frac{2G}{R^+(z_o)}. \tag{13}$$

3 Solution of Canonical Dual Series Equations

Consider the following dual series equations with trigonometric kernel for infinite sequence of coefficients

$$\sum_{n=-\infty}^{\infty} \bar{x}_n |n| e^{in\psi} = F(e^{i\psi}), \quad \psi \in M = (|\psi| < \theta) \tag{14}$$

$$\sum_{n=-\infty}^{\infty} \bar{x}_n e^{in\psi} = 0, \quad \psi \in N = (\theta < |\psi| \leq \pi) \tag{15}$$

where $F(e^{i\psi})$ is a known function with an expansion $F(e^{i\psi}) = \sum_n f_n e^{in\psi}$.

Assuming the series is term-by-term differentiable, we replace (15) with its derivative with respect to ψ and add the identity at $\psi = 0$ to get

$$\sum_{n=-\infty}^{\infty} \bar{x}_n n e^{in\psi} = 0. \tag{16}$$

By introducing functions $X^{\pm}(z)$ of the complex variable $z = e^{i\psi}$ such that

$$X^+(z) = \sum_{n>0} \tilde{x}_n n z^n, \quad |z| \leq 1 \tag{17}$$

$$X^-(z) = -\sum_{n<0} \tilde{x}_n n z^n, \quad |z| \geq 1 \tag{18}$$

we arrive at the functional equations,

$$X^+(e^{i\psi}) + X^-(e^{i\psi}) = F(e^{i\psi}); \quad \psi \in M \tag{19}$$

$$X^+(e^{i\psi}) - X^-(e^{i\psi}) = 0; \quad \psi \in N \tag{20}$$

which constitute the RHP considered above. The determination of the vector $\{\bar{x}_n\}_{n=-\infty}^{\infty}$ is given in detail in [3], so it will not be repeated here. It is considered to be essential to include the final result as

$$\tilde{x}_n = \sum_{n=-\infty}^{\infty} f_n T_{mn}(\cos\theta) \tag{21}$$

where $T_{mn}(u)$ are related to the Legendre polynomials $P_n(u)$ as follows

$$T_{mn}(u) = \begin{cases} Q_{mn}(u), & m \neq 0 \\ Q_{n0}(u), & m = 0, n \neq 0 \\ -\ln[(1+u)/2], & m = n = 0 \end{cases} \tag{22}$$

where

$$Q_{mn}(u) = \frac{1}{2(m-n)}[P_{m-1}(u)P_n(u) - P_m(u)P_{n-1}(u)], \quad m \neq n$$

$$Q_{mm}(u) = \frac{\text{sgn}(m)}{2|m|} \sum_{s=0}^{|m|} q_{|m|-s}(u) P_{|m|-s-1}(u), \quad m \neq 0$$

$$q_o(u) = 1, q_1(u) = -u, ..., q_s(u) = P_s(u) - 2uP_{s-1}(u) + P_{s-2}(u)$$

and we make use of the relation $P_{-s-1}(u) = P_s(u)$.

4 Formulation for E-wave Scattering by Cavity-Backed Apertures

The geometries analyzed are shown in Fig. 1 and 2. The electric field vector of the incident plane wave is taken to be parallel to the axis of the cylinder, and the axial component of the magnetic field is taken to be zero (i.e. TM with respect to the axis of the cylinder). This E-polarized plane wave is assumed to be normally incident on the cylinder; hence the problem is two dimensional. The coordinate system (r, φ, z) is coaxial with the cylinder. The screen which has a radius of "a" is taken to be in the interval of $\theta < |\varphi - \varphi_o| \leq \pi$. The angular width of the slit is 2θ, and the angle between the center of the slit and the x axis is φ_o. The cylindrical cavity is coated with an absorbing material with thickness t. The radius "b" is at either $a - t$ or $a + t$ depending on whether the coating is on the inside or on the outside, respectively. The relative permittivity and permeability of the absorbing material are ε_r and μ_r, respectively. Our objective is to analyze the radar scattering behavior of this geometry for various frequencies. The problem is scalar, so the total field can be characterized by the single E_z component. The time dependence $e^{i\omega t}$ has been assumed and suppressed.

First, consider the geometry shown in Fig. 1. The total field can be expressed as follows

$$E_z(\vec{r}) = \begin{cases} E_z^{in}(\vec{r}) + E_z^{sc}(\vec{r}), & r > a \\ E_z^{sc}(\vec{r}), & b < r < a \\ E_z^{sc}(\vec{r}), & r < b \end{cases} \tag{23}$$

where $E_z^{in}(\vec{r})$ and $E_z^{sc}(\vec{r})$ stand for incident and scattered fields, respectively.

The scattered field E_z^{sc} satisfies the 2-D Helmholtz equations:

$$\begin{aligned} (\nabla^2 + k_o^2)E_z^{sc}(\vec{r}) = 0, & \quad r > a, \ r < b \\ (\nabla^2 + k_o^2\varepsilon_r\mu_r)E_z^{sc}(\vec{r}) = 0, & \quad b < r < a \end{aligned} \tag{24}$$

where $k_o = \omega\sqrt{\mu_o\varepsilon_o}$ is the free-space wave number and ∇^2 is the Laplacian operator.

In addition, we impose the boundary conditions: First, the continuity of E_z on the closed contours $r = a$ as well as $r = b$, and the continuity of H_φ on $r = b$.
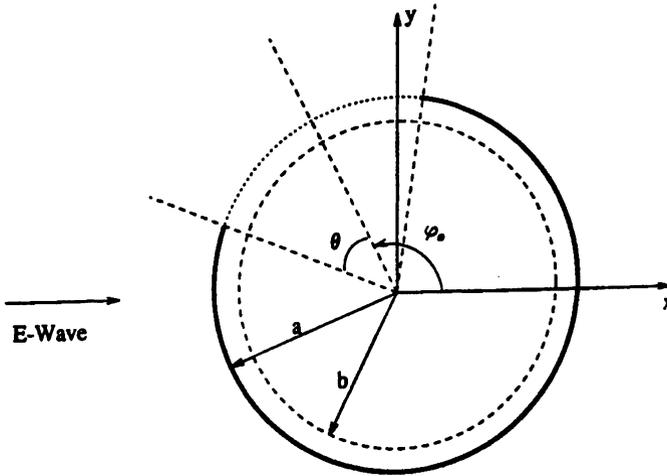

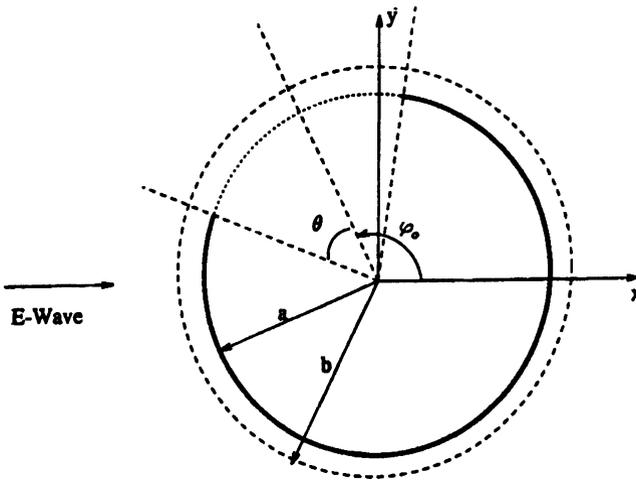**Fig. 1.** *E*-wave scattering by an inner-coated cavity-backed aperture

Fig. 2. *E*-wave scattering by an outer-coated cavity-backed aperture

Second, the continuity of H_φ in the aperture region and vanishing E_z on the screen, at $r = a$.

Because of the sharp edges of the screen, the field should satisfy certain edge conditions. These conditions are satisfied by the requirement that the total electrical and magnetic energy stored inside any finite neighborhood of the edge must be finite. Finally, the Sommerfeld radiation condition should be satisfied far from the scatterer as $r \to \infty$.

5 Derivation of Dual Series Equations

The scattered field expansions in three regions of Fig. 1 are assumed to be

$$E_z^{sc} = \sum_{n=-\infty}^{n=\infty} \begin{cases} A_n H_n(k_o r), & r > a \\ B_n J_n(kr) + C_n H_n(kr), & b < r < a \\ D_n J_n(k_o r), & r < b \end{cases} e^{in\varphi} \tag{25}$$

where $k = k_o \sqrt{\mu_r \varepsilon_r}$, J_n and H_n represent the Bessel and Hankel functions of the first kind and order n, respectively.

The incident plane wave of unit amplitude has the Fourier expansion as

$$E_z^{in} = e^{ik_o x} = e^{ik_o r \cos\varphi} = \sum_{n=-\infty}^{\infty} i^n J_n(k_o r) e^{in\varphi}. \tag{26}$$

The number of unknown coefficients in (25) can be reduced by applying boundary conditions that are valid on the closed contour, that is, the continuity of E_z at $r = a$ and $r = b$ as well as the continuity of H_φ at $r = b$. Hence

$$B_n = \frac{i^n J_n(k_o a) + H_n(k_o a) A_n}{J_n(ka)\xi_n - H_n(ka)\eta_n} \xi_n, \tag{27}$$

$$C_n = -\frac{i^n J_n(k_o a) + H_n(k_o a) A_n}{J_n(ka)\xi_n - H_n(ka)\eta_n} \eta_n, \tag{28}$$

and

$$D_n = \frac{2i}{\pi k_o b \mu_r} \frac{i^n J_n(k_o a) + H_n(k_o a) A_n}{J_n(ka)\xi_n - H_n(ka)\eta_n} \tag{29}$$

are obtained. In (27), (28) and (29)

$$\xi_n = \sqrt{\frac{\varepsilon_r}{\mu_r}} H_n'(kb) J_n(k_o b) - H_n(kb) J_n'(k_o b)$$

and prime denotes derivative with respect to the argument.

Zero value of E_z on the screen and the continuity of H_φ in the aperture lead to dual series equations for the expansion coefficients

$$\sum_{n=-\infty}^{\infty} x_n \gamma_n e^{in\varphi} = -\sum_{n=-\infty}^{\infty} d_n e^{in\varphi}, \qquad |\varphi - \varphi_o| < \theta \tag{30}$$

$$\sum_{n=-\infty}^{\infty} x_n e^{in\varphi} = 0, \qquad \theta < |\varphi - \varphi_o| \le \pi \tag{31}$$

where

$$x_n = i^n J_n(k_o a) + H_n(k_o a) A_n \ , \tag{32}$$

$$d_n = -\frac{2i^{n+1}}{\pi k_o a H_n(k_o a)} \tag{33}$$

and

$$\gamma_n = \frac{H_n'(k_o a)}{H_n(k_o a)} - \sqrt{\frac{\varepsilon_r}{\mu_r}} \ \frac{J_n'(ka)\xi_n - H_n'(ka)\eta_n}{J_n(ka)\xi_n - H_n(ka)\eta_n} \ . \tag{34}$$

Investigating the asymptotic behaviour of γ_n as $|n| \to \infty$, based on the corresponding expressions for cylindrical functions [13], we find

$$\gamma_n \sim \frac{|n|}{k_o a}(1 + \frac{\beta_n}{\mu_r}) \tag{35}$$

where

$$\beta_n = 1 + 2\frac{\mu_r - 1}{\mu_r + 1}\left(\frac{b}{a}\right)^{2n}\left[1 - \frac{\mu_r - 1}{\mu_r + 1}\left(\frac{b}{a}\right)^{2n}\right]^{-1} . \tag{36}$$

For $b \ne a$, the dominant term in (36) is the first term, which is 1. The remaining terms decrease very fast as n increases.

Adding and subtracting the asymptotic expression (35) from γ_n in (30), we get the following result

$$\sum_{n=-\infty}^{\infty} x_n |n| e^{in\varphi} = \sum_{n=-\infty}^{\infty} (x_n \Delta_n + \frac{\mu_r k_o a}{\mu_r + 1} d_n)e^{in\varphi}, \qquad |\varphi - \varphi_o| < \theta \tag{37}$$

where

$$\Delta_n = \frac{\mu_r k_o a}{\mu_r + 1}\gamma_n + |n| , \tag{38}$$

x_n and d_n are given in (32) and (33), respectively. Equation (37) and (31) form canonical dual series equations as shown above in (14) and(16). The solution of this dual series equations is given as described above. By defining

x_n and d_n are given in (32) and (33), respectively. Equation (37) and (31) form canonical dual series equations as shown above in (14) and (16). The solution of this dual series equations is given as described above. By defining

$$\rho_n = A_n / J_n(k_o a) , \tag{39}$$

one can write (21) as

$$\rho_m = \sum_{n=-\infty}^{\infty} K_{mn} \rho_n + S_m, \quad m = 0, \pm 1, \dots \tag{40}$$

where

$$K_{mn} = \frac{H_n(k_o a) J_n(k_o a)}{H_m(k_o a) J_m(k_o a)} \Delta_n W_{mn}, \tag{41}$$

$$S_m = \frac{-i^m}{H_m(k_o a)} + \frac{1}{H_m(k_o a) J_m(k_o a)}$$

$$\times \sum_{n=-\infty}^{\infty} i^n \left[J_n(k_o a) \Delta_n - \frac{2i\mu_r(\mu_r+1)^{-1}}{\pi H_n(k_o a)} \right] W_{mn} \tag{42}$$

and

$$W_{mn} = e^{i(n-m)\varphi_o} T_{mn}(\cos\theta) . \tag{43}$$

The coefficients W_{mn} contain all the information about the angular geometry of the screen, as functions of θ and φ_o. Expression (40) can be written as a single operator equation

$$(I - K)\rho = S \tag{44}$$

where $\rho = \{\rho\}_{n=-\infty}^{\infty}$, I is identity matrix and $K = \{K_{mn}\}_{m,n=-\infty}^{\infty}$. Operator K can be shown (see [3] to be compact in the Hilbert space of l_2 ($\rho \in l_2$ if $\sum_{n=-\infty}^{\infty} |\rho_n|^2 < \infty$). Besides, vector $S = \{S_m\}_{m=-\infty}^{\infty} \in l_2$ as well. It means that (44) is a regularized operator equation, and therefore well known Fredholm's theorems are valid [14]: solution ρ does exist and is unique. Moreover, any solution of (44) can be shown (see [3]) to satisfy

$$\sum_{n=-\infty}^{\infty} |\rho_n|^2 |n+1| < \infty \tag{45}$$

as ρ_n decay as $O(n^{-3/2})$ when $|n| \to \infty$. Hence, (45) ensures the validity of the edge condition [3]. Further, this solution can be approximated with any desired accuracy by means of truncation of the matrix $K = \{K_{mn}\}_{m,n=-\infty}^{\infty}$, and vector $S = \{S_m\}_{m=-\infty}^{\infty}$ for all $|m|, |n| > N_{tr}$.

verified. To provide an accuracy of 0.1%, we had to take $N_{tr} =$ integer part of $(k_o a)+15$. It is noted that, all the field coefficients in (25), namely A_n, B_n, C_n and D_n are calculated using equations (39), (27), (28) and (29), respectively.

We treat the second problem (for the outer covering) in a similar way. In (25), we replace a's with b's; afterwards the same procedure is followed. The resultant infinite system of linear equations is formally the same as that of the previous problem (40). It is rewritten below for convenience

$$\rho_m = \sum_{(n)} K_{mn}\rho_n + S_m, \quad m = 0,\pm 1,... \qquad (46)$$

where now

$$K_{mn} = \frac{J_n(k_o a)}{J_m(k_o a)} \frac{H_n(ka)\xi_n - J_n(ka)\eta_n}{H_m(ka)\xi_m - J_m(ka)\eta_m} \Delta_n W_{mn}, \qquad (47)$$

and the coefficients are

$$\xi_n = J_n(kb)H_n'(k_o b) - \sqrt{\frac{\varepsilon_r}{\mu_r}} J_n'(kb) H_n(k_o b)$$

$$\eta_n = H_n(kb)H_n'(k_o b) - \sqrt{\frac{\varepsilon_r}{\mu_r}} H_n'(kb) H_n(k_o b)$$

and

$$\Delta_n = -\frac{\mu_r k_o a}{\mu_r + 1}\gamma_n + |n| \qquad (48)$$

where

$$\gamma_n = \frac{J_n'(k_o a)}{J_n(k_o a)} - \sqrt{\frac{\varepsilon_r}{\mu_r}} \frac{H_n'(ka)\xi_n - J_n'(ka)\eta_n}{H_n(ka)\xi_n - J_n(ka)\eta_n} \quad .$$

Coefficient S_m in (46) is now given by

$$S_m = e_m \left\{ g_m + \sum_{n=-\infty}^{\infty} i^n \{h_n\Delta_n + 8ia^{-1}l_n\}W_{mn} \right\} \qquad (49)$$

where

$$e_m = \frac{1}{J_m(k_o a)[H_m(ka)\xi_m - J_m(ka)\eta_m]}$$

$$g_m = -i^m[H_m(ka)s_{2m} - J_m(ka)s_{4m}]$$

$$h_n = H_n(ka)s_{2n} - J_n(ka)s_{4n}$$

$$l_n = [H_n(ka)\xi_n - J_n(ka)\eta_n]^{-1}$$

$$a = \pi^3 (k_o b)^2 \mu_r (\mu_r + 1)$$

$$s_{2n} = J_n(kb) J'_n(k_o b) - \sqrt{\frac{\varepsilon_r}{\mu_r}} J'_n(kb) J_n(k_o b),$$

$$s_{4n} = H_n(kb) J'_n(k_o b) - \sqrt{\frac{\varepsilon_r}{\mu_r}} H'_n(kb) J_n(k_o b).$$

The second problem has the same type of operator equation as the previous one.

6 Numerical Results and Discussions

Numerical results are obtained for the radar cross section (RCS) behaviour of a CBA which is coated either from inside or from outside with absorbing materials. The formula for RCS can be written in terms of expansion coefficients as

$$\sigma_{bs} = \frac{4}{k_o} \left| \sum_{-N_{tr}}^{N_{tr}} \rho_n i^n J_n(k_o a) \right|^2 .$$

We normalized RCS with respect to πa which is the geometrical optics value for the perfectly conducting closed circular cylinder. The normalized RCS results are presented in Figs. 3a to 4b as a function of frequency for different coating materials and different orientations of the aperture. In all figures, θ is taken as 30°, and the materials used for coating are shellac, natural XL ($\varepsilon_r = 3.45 + 0.25i$, $\mu_r = 1$) (dashed curves) and poly-2.5-dichlorostyrene ($\varepsilon_r = 7.3$, $\mu_r = 0.91 + 0.32i$) (solid curves). The thickness of the absorbing layer is 10% of the radius of the screen. For comparison, dotted curves represent the RCS calculated for the same CBA without any coating, and dash-dotted line in Fig. 3b gives the RCS of a perfectly conducting circular cylinder. It is noted that for $\varphi_o = 180^o$ case, the average level of RCS of uncoated CBA is much higher than that of closed uncoated circular cylinder of the same radius (See Fig. 3b). In addition, strong resonances are observed in the RCS. The resonances are due to the excitation of the damped natural modes of the screen as a cavity-backed aperture.

The effect of the presence of the absorbing material on the outer and inner wall of CBA are demonstrated in Figs. 3a and 3b, respectively for the case of aperture in the illumination region. As observed in these figures, the lowest order peak cannot be reduced by using absorbing dielectric material. However, when the frequency increases, the resonance peaks are reduced. It is due to the fact that low frequency E-field has zero value on the screen and has a maximum on the axis of the cylinder, as zeroth harmonic is dominating. But when the frequency is increased, the number of azimuthal harmonics of comparable amplitude also increases and the location of the maximum of E-field moves away from the axis.
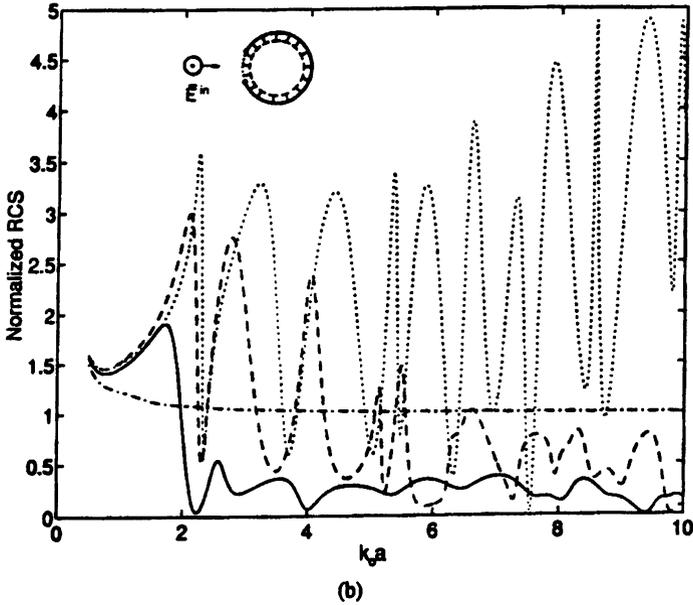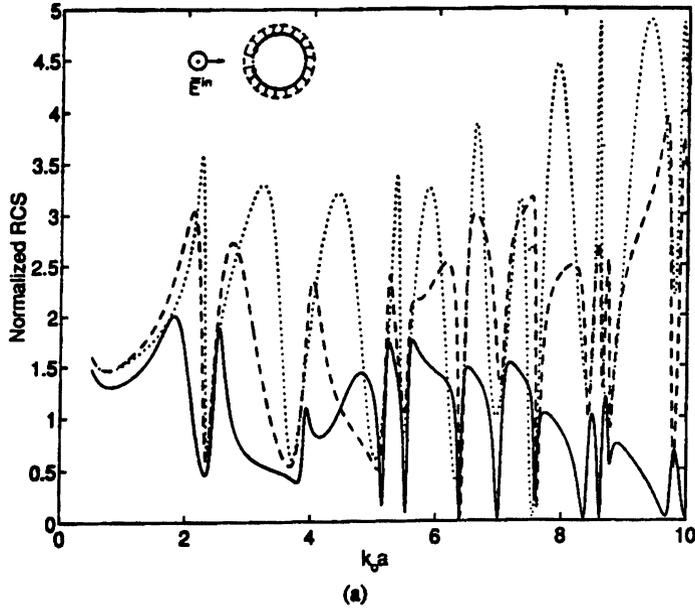
Fig. 3. The normalized RCS of (a) an uncoated and outer-coated CBA (coating radius $b = 1.1a$) and (b) an unslitted cylinder, uncoated and inner-coated CBA (coating radius $b = 0.9a$) for two different absorbing materials with CBA having 60° aperture size and $\varphi_o = 180^o$. Solid line, $\varepsilon_r = 7.3$, $\mu_r = 0.91 + 0.32i$; dashed line, $\varepsilon_r = 3.45 + 0.25i$, $\mu_r = 1$; dotted line, uncoated cylinder, i.e., $\varepsilon_r = 1$, $\mu_r = 1$; dot-dashed line, unslitted cylinder
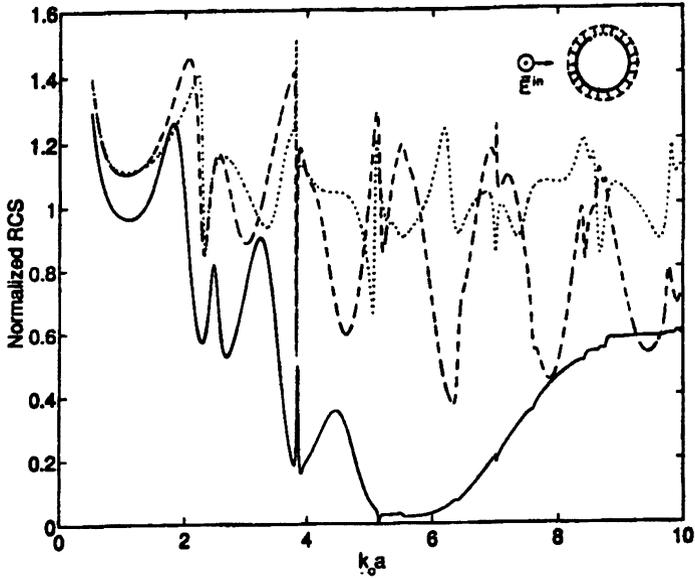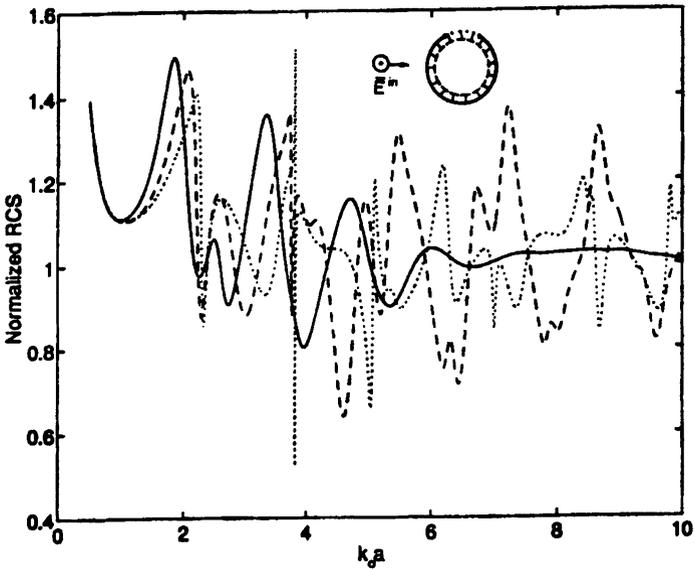
Fig. 4. The normalized RCS of (a) an uncoated and outer-coated CBA (coating radius $b = 1.1a$) and (b) an uncoated and inner-coated CBA (coating radius $b = 0.9a$) for two different absorbing materials with CBA having $60°$ aperture size and $\varphi_o = 90^o$. Solid line, $\varepsilon_r = 7.3$, $\mu_r = 0.91 + 0.32i$; dashed line, $\varepsilon_r = 3.45 + 0.25i$, $\mu_r = 1$; dotted line, uncoated cylinder, i.e., $\varepsilon_r = 1$, $\mu_r = 1$

Therefore, resonances of higher order modes can be suppressed by coating the screen with the absorbing material from inside. To reduce the lowest order resonance peak, one needs to use magnetic absorbing material as seen in Fig. 3a and 3b. Since the magnetic field has an azimuthal component, which is not zero on the screen, it can be suppressed by using lossy magnetic material which results in a lower back scattered power. Coating from outside has no effect on the internal resonances but it helps only to decrease the amplitude of the incident field entering into cavity. Therefore, the sharp minima cannot be suppressed, but the average level of RCS is reduced as seen in Fig. 3a. So the resonances are just shifted in frequency but they are still sharp which may cause the target to be easily identified.

As an example of nonsymmetrical excitation, we examine the case of 90° orientation, i.e. when the aperture is looking up. Coating from outside is much effective for reducing the average level of the RCS, but there are still sharp resonances (See Fig. 4a). The frequency value at which RCS has a broad minimum in those figures corresponds to the frequency at which the reflection coefficient is minimum for quarter-wavelength magneto-dielectric coating on a perfectly conducting plane. If the coating is from outside, some of the energy is absorbed by the coating material. So, the amplitudes of the resonance peaks are reduced. On the other hand, as seen in Fig. 4b, coating from inside is again effective for suppressing the resonances, except the lowest one. The resonance phenomena are greatly reduced if the frequency is increased and magnetic coating is used.

The results obtained for the case when the aperture is in the shadow region are very similar to the closed cylinder case (See Fig. 3b, dash-dotted curves). This happens because the E-polarized excitation induces only longitudinal current on a cylindrical scatterer, hardly reaching the shadow part of surface, and hence, not exciting the interior of CBA.

7   Conclusions

The method of regularization is introduced and its application through Riemann-Hilbert problem technique for electromagnetic problems is discussed. The method converts the integral operator into a form for which the existence of the solution is guaranteed and numerical approximation is mathematically rigorous.

The method is applied to the RCS study of coated cavity-backed apertures. The problem is first formulated in dual series equations and then solved by using RHP technique. According to the numerical results, one can say that it is much more preferable to choose a lossy magnetic material for coating. Further, it is much better to make the coating from the inside to suppress the resonances when the interior resonance is the dominant feature in the backscattering characteristics. Moreover, in case of direct on-aperture incidence, the inner covering is obviously better for any frequency. Otherwise, coating from the outside can also be preferable to reduce the average level of the RCS off the resonant frequency.

References

[1] K. Kobayashi, and A. Sawai, "Plane Wave Diffraction by an Open-Ended Parallel-Plate Waveguide Cavity," *J. Electromag. Waves Appl.*, vol. 6, pp. 475-512, 1992.

[2] Z. S. Agranovich, V. A. Marchenko and V. P. Shestopalov, "Diffraction of a Plane Electromagnetic Wave from Plane Metallic Lattices," *Soviet Physics-Tech. Physics.*, vol. 7, pp. 277-286, 1962.

[3] A. I. Nosich, "Green's Function-Dual Series Approach in Wave Scattering by Combined Resonant Scatterers," in M. Hashimoto, M. Idemen and O. A. Tretyakov (eds.), *Analytical and Numerical Methods in EM Wave Theory*, Tokyo, Science House, pp. 419-469, 1992.

[4] A. I. Nosich, *Electromagnetic Characterization of Unclosed Circular Cylindrical Screens*, Ph.D. Dissertation, Kharkov University, 1979 (in Russian).

[5] R. W. Ziolkowski, "N-series Problems and the Coupling of Electromagnetic Waves to Apertures: A Riemann-Hilbert Approach," *Soc. Industrial Appl. Math.*, vol. 16, no. 2, 1985.

[6] R. W. Ziolkowski and J. B. Grant, "Scattering from Cavity-Backed Apertures: The Generalized Dual Series Solution of the Concentrically Loaded E-Pol Slit Cylinder Problem," *IEEE Trans. Antennas Propagat.*, vol. 35, no. 5, pp. 504-528, May 1987.

[7] W. A. Johnson and R. W. Ziolkowski, "The Scattering of an H-Polarized Plane Wave from an Axially Slotted Infinite Cylinder: A Dual Series Approach," *Radio Science*, vol. 19, no.1, pp. 275-291, Jan. 1984.

[8] D. Colak, A. I. Nosich and A. Altintas, "RCS Study of Cylindrical Cavity-Backed Apertures with Outer or Inner Material Coating: The Case of E-Polarization," *IEEE Trans. Antennas Propagat.*, vol. 41, no.11, pp. 1551-1559, Nov. 1993.

[9] D. Colak, A. I. Nosich and A. Altintas, "RCS Study of Cylindrical Cavity-Backed Apertures with Outer or Inner Material Coating: The Case of H-Polarization," *IEEE Trans. Antennas Propagat.*, vol. 43, no. 5, pp. 440-447, May 1995.

[10] T. Oguzer, A. Altintas, and A. I. Nosich, "Accurate Simulation of Reflector Antennas by the Complex-Source Dual-Series Approach," *IEEE Trans. Antennas Propagat.*, vol. 43, no. 8, pp. 793-801, Aug. 1995.

[11] A. I. Nosich, V. B. Yurchenko and A. Altintas, "Numerically Exact Analysis of a Two-Dimensional Variable-Resistivity Reflector Fed by a Complex-Point Source," *IEEE Trans. Antennas Propagat.*, vol. 45, no. 11, pp. 1592-1601, Nov. 1997.

[12] S. Koshikawa, D. Colak, A. Altintas, K. Kobayashi and A. I. Nosich, "A Comparative Study of RCS Predictions of Canonical Rectangular and Circular Cavities with Double-Layer Material Loading," *IEICE Trans. Electron.*, vol. E80-C, pp. 1457-1466, Nov. 1997.

[13] M. Abramowitz and I. A. Stegun, *Handbook of Mathematical Functions*, New York: Dover, 1965

[14] P. M. Morse and H. Feshbach, *Methods of Theoretical Physics*, vol. 1, New York: McGraw-Hill, 1953, sec. 8.2, pp. 907-925.